Chinese Journal of Aeronautics, 2013,26(2): 319–325

Chinese Society of Aeronautics and Astronautics
& Beihang University

Chinese Journal of Aeronautics

cja@buaa.edu.cn
www.sciencedirect.com

Design and simulation of ex-range gliding wing of high altitude air-launched autonomous underwater vehicles based on SIMULINK

Pan Changjun, Guo Yingqing *

School of Power and Energy, Northwestern Polytechnical University, Xi'an 710072, China

Received 23 December 2011; revised 20 February 2012; accepted 6 July 2012
Available online 6 March 2013

KEYWORDS

Autonomous underwater vehicles;
Air launch;
Design;
Simulation;
Wings

Abstract High altitude air-launched autonomous underwater vehicle (AL-AUV) is a new anti-submarine field, which is designed on the Lockheed Martin's high altitude anti-submarine warfare weapons concept (HAAWC) and conducts the basic aerodynamic feasibility in a series of wind tunnel trials. The AL-AUV is composed of a traditional torpedo-like AUV, an additional ex-range gliding wings unit and a descending parachute unit. In order to accurately and conveniently investigate the dynamic and static characteristic of high altitude AL-AUV, a simulation platform is established based on MATLAB/SIMULINK and an AUV 6DOF (Degree of Freedom) dynamic model. Executing the simulation platform for different wing's parameters and initial fixing angle, a set of AUV gliding data is generated. Analyzing the recorded simulation result, the velocity and pitch characteristics of AL-AUV deployed at varying wing areas and initial setting angle, the optimal wing area is selected for specific AUV model. Then the comparative simulations of AL-AUV with the selected wings are completed, which simulate the AUV gliding through idealized windless air environment and gliding with Dryden wind influence. The result indicates that the method of wing design and simulation with the simulation platform based on SIMULINK is accurately effective and suitable to be widely employed.

1. Introduction

Autonomous underwater vehicle (AUV) is un-tethered mobile platform used for survey operation by ocean scientists, marine industry and the military.[1,2] For its ability of accessing otherwise inaccessible regions, lower cost of operation, improved data quality and the ability to acquire nearly synoptic observations of processes in the water, AUV is widely used in ocean investigation. Almost all the dominant countries have paid more and more attention to the AUV technology, which develops rapidly. However, the ability specifically flexibility of the traditional AUV deployed from a water surface vehicle or

* Corresponding author. Tel.: +86 29 88492749.
E-mail addresses: panchangjun@mail.nwpu.edu.cn (C. Pan), yqguo@nwpu.edu.cn (Y. Guo).

Peer review under responsibility of Editorial Committee of CJA.

Production and hosting by Elsevier

1000-9361
http://dx.doi.org/10.1016/j.cja.2013.02.008

sub-marine vehicle is extremely limited by its launching platform's low moving velocity. To promote the application and the ability of AUV's reaching the assigned investigating ocean region, and with the development of aerial vehicle and the airdrop technology, air-launched AUV (AL-AUV) was designed and well developed. Lockheed Martin manufactured air-deployable AUV, MK39 expendable mobile anti-submarine warfare training target (EMATT). Woods Hole Oceanographic Institution (WHOI) designed a set of air-dropped AUV, remote environmental monitoring units (REMUS), and the relational underwater modeling, control and simulation technology of air-launched REMUS AUV[3] and water impact of REMUS AUV dropped in free-fall from a helicopter in a low hover were developed and experimentally analyzed.[4]

Most of the existing air-deployed AUVs only permit to be dropped at low altitude and speed, or launched at high hover above the survey water field and decelerated by parachute, which lack controllability and flexibility. And for military purpose the carrier aircraft of AUV or torpedo is easy to be detected and attacked. Hence, the high altitude anti-submarine warfare weapon conception (HAAWC) was proposed in 2006 by American Navy and experimented by Lockheed Martin manufactured with MK54 torpedo and a LongShot wing unit, launched at 20000 ft (1 ft = 304.8 mm), proving the feasibility and advantage of this conception.[5–8] Meanwhile, the British developed similar high altitude air-launched technology.[9,10] In our country, Northwestern Polytechnical University firstly carried out the high altitude gliding torpedo relative research, analyzed the key technology of trajectory simulation,[11] and calculated the aerodynamic characteristic of torpedo with gliding wing unit[12] and the impact dynamic of air launched torpedo with water.[13,14]

In this paper, a simulation platform of AL-AUV with a pair of ex-range wings and a descending parachute unit is introduced. The usage of wing enables the AUV to be dropped at high altitude and glide a long distance to reach the signed investigating ocean field. The gliding of the AL-AUV with varying wings area and fitting angle is simulated using the simulation platform. And the characteristics of the simulated AL-AUV with varying wings are recorded and analyzed. Concerting the AUV gliding dynamic characteristic and the wing's ability of extending range, the optimal wing area and fitting angle are selected for specific AUV model. The overall design of high altitude AL-AUV has been discussed in Ref. [15].

2. Summary of high altitude AL-AUV

The high altitude AL-AUV investigated in the following description is composed of traditional torpedo-like AUV with hull structure of the REMUS,[16] a pair of ex-range gliding wings unit loaded on the AUV geometrical center with the NACA Clark YH cross section, and a Dohher rotating circular parachute unit at the tail of AUV to decelerate the AUV velocity of water entry. The usage of ex-range gliding wing enables the AL-AUV to be launched at high altitude and glide a long distance from launch point to water entry point. The controllable surface on wings and rudders at AUV tail enhances the AL-AUV's maneuverability, controllability and the ability of anti-interfere caused by environment wind at gliding stage through air. As shown in Fig. 1, the trajectory of high altitude AL-AUV is divided into five stages:

(1) AUV initialization and deployment.
(2) Gliding steadily through air with ex-range wings.
(3) Wings releasing and parachute inflating.
(4) Water entry and parachute releasing.
(5) Moving underwater autonomously.

3. 6DOF dynamic model

The 6DOF motion equation is generally written in the matrix form:

$$\boldsymbol{M}\dot{\boldsymbol{V}} + \boldsymbol{C}(\boldsymbol{V}) \cdot \boldsymbol{V} = \boldsymbol{F} \tag{1}$$

where $\boldsymbol{M}$ is the AL-AUV generalized mass-inertia matrix, $\boldsymbol{C}(\boldsymbol{V})$ the Coriolis-Centripetal (CC) matrix, $\boldsymbol{V}$ the generalized velocity vector involving linear velocity in body fixed frame $\boldsymbol{V}_B = [u\ v\ w]^T$ and angular velocity of body fixed frame relative to the earth inertial frame $\boldsymbol{\Omega}_B = [p\ q\ r]^T$, and $\boldsymbol{F}$ is generalized external force and moment vector acting on AUV in body fixed frame caused by aerodynamics and gravity. Since the origin of body fixed frame is not coincident with the AUV's gravity center, the inertial force and moment acting on AUV will cause

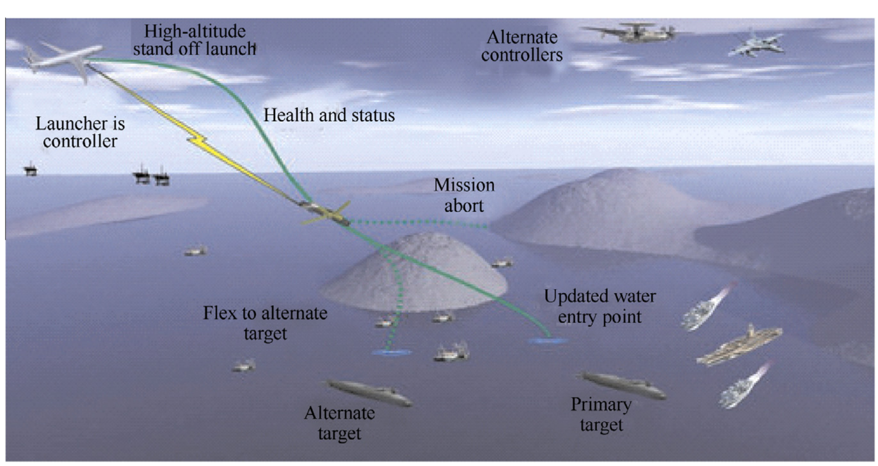

Fig. 1 Image trajectory map of the investigated AL-AUV.

additional structure coupling, and the mass matrix $\boldsymbol{M}$ and CC matrix $\boldsymbol{C}(\boldsymbol{V})$ could be expressed as[17]

$$M = \begin{bmatrix} m\boldsymbol{I}_{3\times3} & -m\boldsymbol{S}(\boldsymbol{r}_g) \\ m\boldsymbol{S}(\boldsymbol{r}_g) & \boldsymbol{I}_0 \end{bmatrix} \tag{2}$$

$$\boldsymbol{C}(\boldsymbol{V}) = \begin{bmatrix} m\boldsymbol{S}(\boldsymbol{\Omega}_B) & -m\boldsymbol{S}(\boldsymbol{\Omega}_B)\boldsymbol{S}(\boldsymbol{r}_g) \\ m\boldsymbol{S}(\boldsymbol{r}_g)\boldsymbol{S}(\boldsymbol{\Omega}_B) & -\boldsymbol{S}(\boldsymbol{I}_0\boldsymbol{\Omega}_B) \end{bmatrix} \tag{3}$$

where $\boldsymbol{I}_{3\times3}$ is an unity matrix, $\boldsymbol{I}_0$ the AUV inertial matrix, m the AUV mass and $\boldsymbol{r}_g$ the position vector of gravity center with respect to frame origin center. The matrix $\boldsymbol{S}(*)$ is a skew-symmetrical matrix[18] that transfers vector cross product to matrix form.

Defining absolute velocity $V = |\boldsymbol{V}|$, the generalized force and moment vector $\boldsymbol{F}$ acting on AUV due to aerodynamic and gravity with respect to the body fixed frame is partitioned as

$$\boldsymbol{F} = \boldsymbol{F}_d(V, \alpha, \beta) + \boldsymbol{F}_f(V, \alpha, \beta) + \boldsymbol{F}_{hy}(\Theta_B) + \boldsymbol{F}_w(V, \alpha, \alpha_{set}) \tag{4}$$

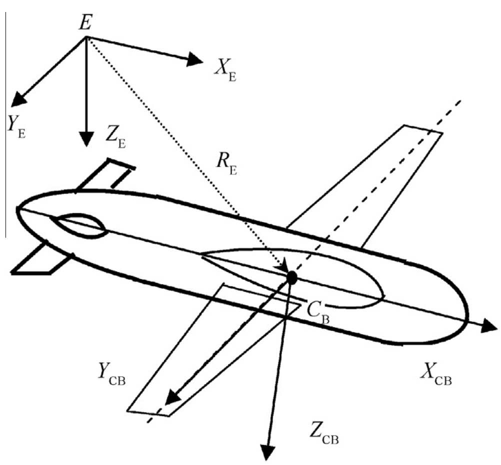

Fig. 2 Coordinate and structure of AL-AUV.

where $\boldsymbol{F}_d$ and $\boldsymbol{F}_f$ are velocity dependent aerodynamic force and moment respectively acting on AUV body and fins; $\boldsymbol{F}_{hy}$ represents the gravity inter force and moment in the body-fixed frame; $\boldsymbol{F}_w$ is the wing lift and drag force and moment vector, and α, β, Θ_B, α_{set} respectively denote AUV angle of attack, slide angle, pitch altitude angle and wings' setting angle which is defined with the angle between the AUV x-axis and the wing cross section chord.

Modeling AL-AUV as a rigid body, two coordinates are defined in Fig. 2, an earth fixed inertial frame with relevant quantities exhibiting a subscript "E" and an AUV body fixed frame with the alternative subscript "B". The transformation matrixes of the related translational velocity component between two coordinate systems and the angular velocity relative to the body fixed frame are given with Eq. (5).

$$\dot{\boldsymbol{R}}_E = \boldsymbol{C}_B^E \cdot \boldsymbol{V}_B \text{ and } \dot{\boldsymbol{Eu}}_E = \boldsymbol{\eta}_B^E \cdot \boldsymbol{\Omega}_B \tag{5}$$

where $\dot{\boldsymbol{R}}_E$ and $\dot{\boldsymbol{Eu}}_E$ respectively represent the variation rate of AUV position and attitude in earth fixed frame; $\boldsymbol{C}_B^E$ and $\boldsymbol{\eta}_B^E$ respectively denote linear and angular transform matrix.

With all the above dynamics, motion and kinematics equations, a simulation system is designed and established using MATLAB/SIMULINK block.

4. Simulation platform based on SIMULINK

Since the high altitude AL-AUV's gliding stage is highly similar to unmanned aerial vehicle (UAV), the establishment of simulation platform based on SIMULINK can use the method of modeling and simulation used in aeronautic control for references.[19,20] Hence the high altitude AL-AUV simulation platform as shown in Fig. 3 comprises four modules, navigation and guidance block, GPS sensor block, controller block and 6DOF dynamic model block.

The AL-AUV 6DOF dynamic model block, Fig. 4, consists of four sub-modules. The aero/hydro-dynamic force and moment sub-module (see Fig. 5) calculates the aero/hydro-dynamic effect on AUV body, wings and fins in body fixed frame. The environment model (see Fig. 6) sub-module adds

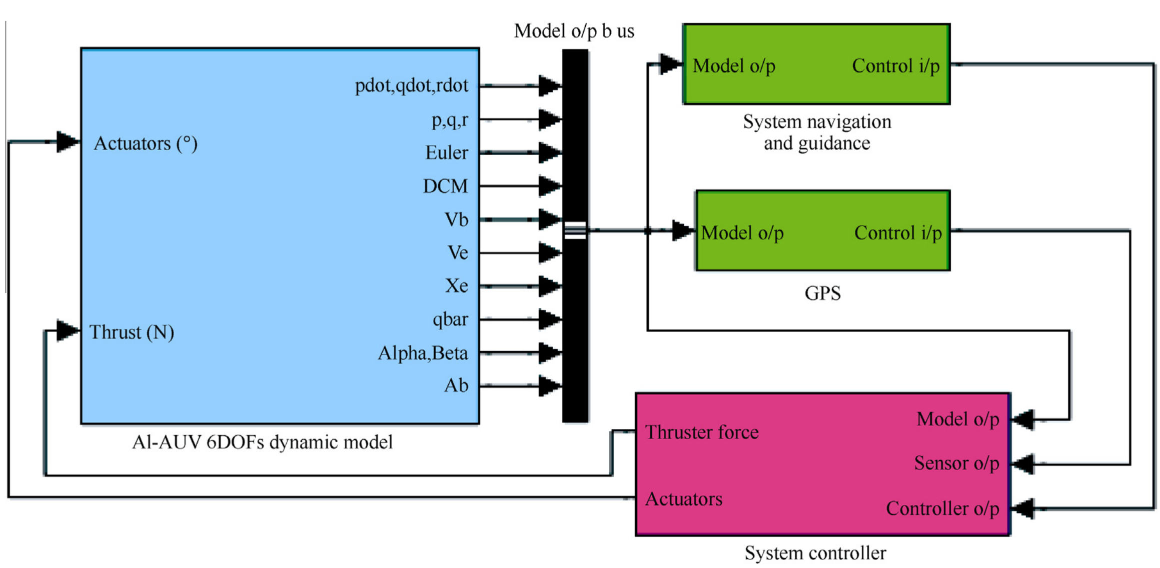

Fig. 3 High altitude AL-AUV simulation platform.

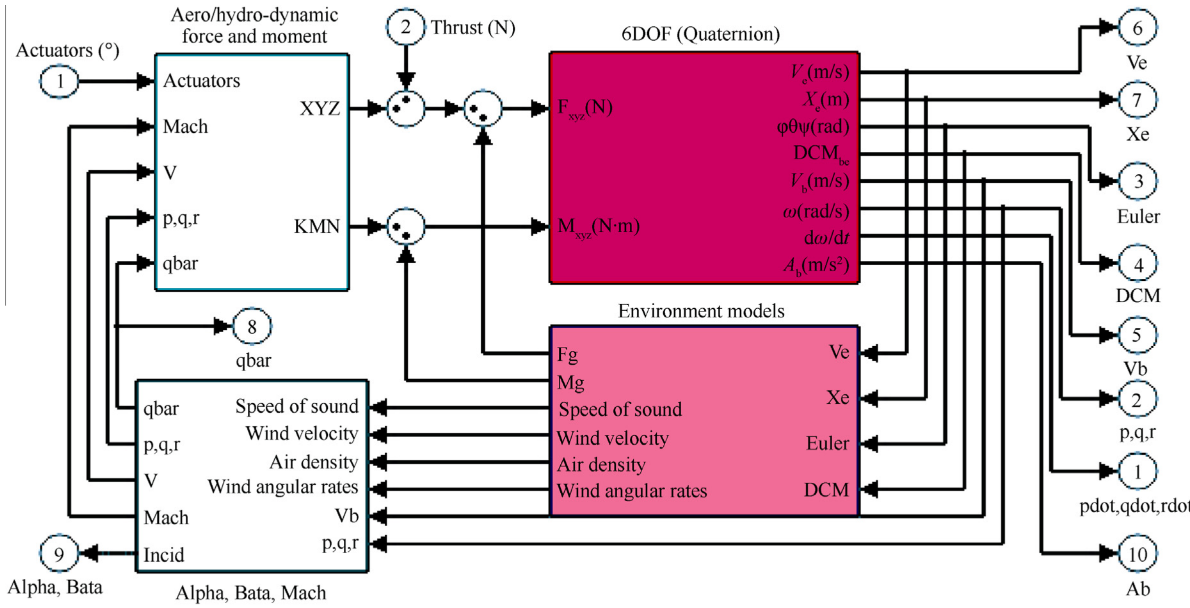

Fig. 4 AL-AUV 6DOF dynamic model sub-module.

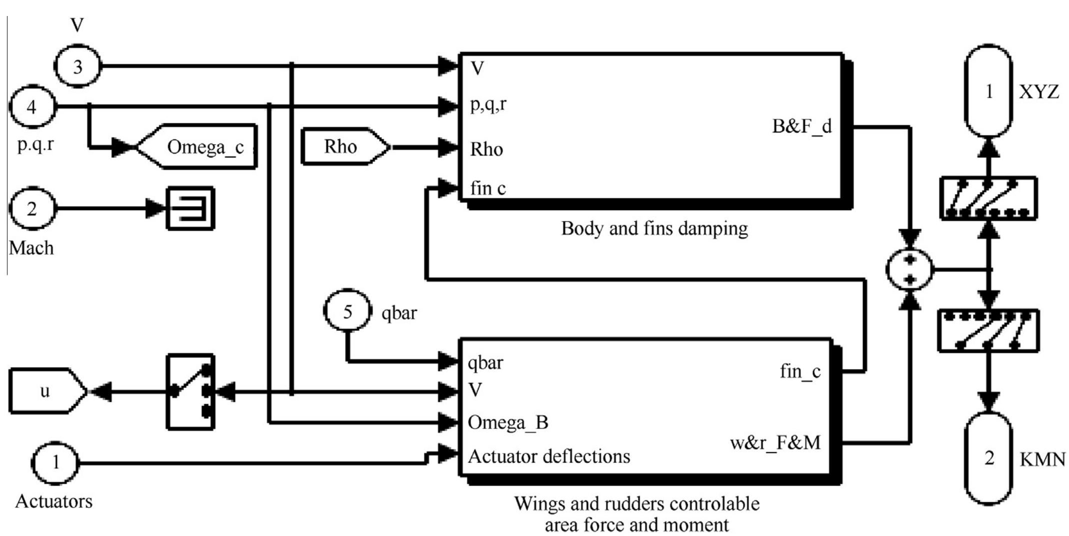

Fig. 5 Dynamic force and moment sub-module.

atmosphere and wind influence to system aerodynamic calculation and height effect to gravity acceleration. The 6DOF (Quaternion) sub-module processes motion and kinematics equations provided in Section 3. And an Alpha Beta Mach module calculates the AUV moving angle of attack in different frame planes.

Compile MATLAB program to evaluate the parameters needed in AUV aerodynamic effect calculation and initialize the launching environment condition and the AUV initial moving state, position and attitude state, and then set appropriate simulation time and step and execute the platform. Then the AL-AUV gliding dynamic data will be put in MATLAB workspace. Then analyze the obtained simulation data, the dynamic characteristics of AL-AUV with varying wing parameters will be achieved, which will be deeply discussed in Section 5.1.

5. Simulation and conclusions

The AL-AUV aerodynamic force and moment Eq. (4) indicates that the steady gliding state, especially the gliding angle of attack (α, β) and attitude pitch angle Θ_B, for a specific AUV is due to the area and the initial setting angle of wings. Multi-executing the simulation system with varying wing area and setting angle and analyzing the simulated gliding data, the effect of wing parameter and initial launching condition on steady gliding state was well investigated.

The simulated AL-AUV was designed based on REMUS-100 AUV with structure parameters (see Table 1). The AUV dynamic non-dimensional coefficients used in aerodynamic calculation of the above simulation platform were provided in Ref. [16].

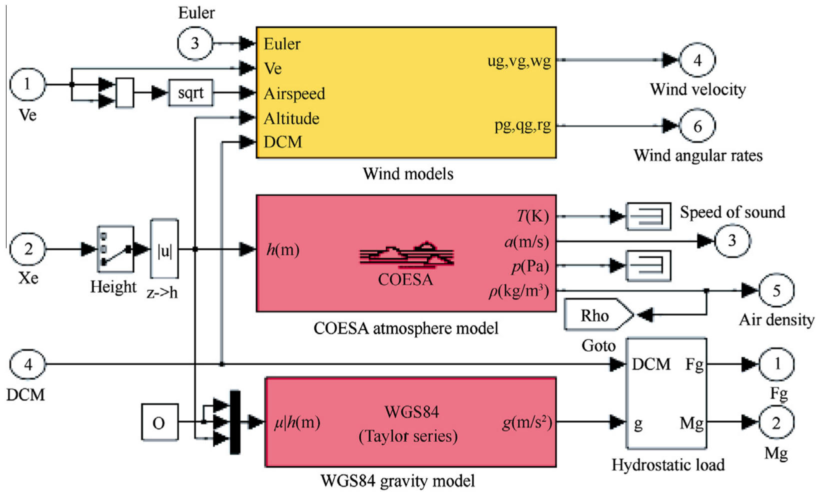

Fig. 6 Environment model sub-module.

Table 1 AL-AUV parameters.

Parameter	Value	Unit	Description
l	1.33	m	Total length of AUV
R	9.55	cm	AUV maximum hull radius
A_p	0.226	m^2	Hull projected area
W	299	N	Estimated weight

Table 2 Initial conditions.

Parameter	Range or value	Step	Description
S_w/S_0	[0.2 1]	0.1	Ratio of selected wing area to reference wing area
α_{set} (°)	[0 4]	0.1	Wing initial fix angle
V (m/s)	75		Launching speed
H (m)	2000		Launching altitude

5.1. Wing design and optimization

To simplify the simulation calculation and save the simulation time, the 3D (x, z and pitch) motion simulation with idealized windless environment was processed at this wing selection stage. Set the initial conditions as Table 2 and multi-executed the simulation platform for 100 s, the following corresponding relative figures of steady gliding altitude, attack angle and wing area, as well as initial setting angle were obtained (see Fig. 7).

Fig. 7(a) and (b) show the variations of AUV gliding angle of attack α and pitch angle Θ_B with the change of wing setting angle α_{set} and time for specific wing area. The figures show that angles α and Θ_B were steady after about 40 s damping, and indicate that the AL-AUV with ex-range wing is large-range stable and α_{set} affects AL-AUV's dynamic characteristic and determines AUV's steady gliding angle of attack and pitch angle for the specific wing area. The corresponding relations of steady α, Θ_B and α_{set} for different wing areas are shown in Fig. 7(c) and (d), with arrow labeled wing areas' increase or decrease.

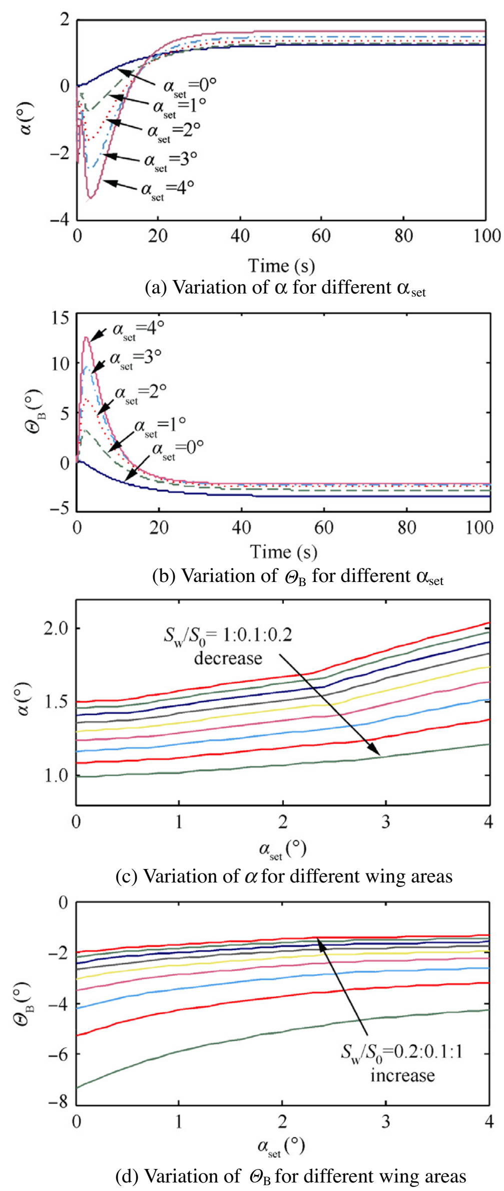

Fig. 7 Variation of α and Θ_B.

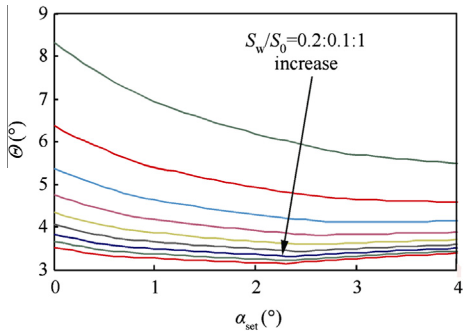

Fig. 8 Variation of gliding angles with α_{set} for different wing areas.

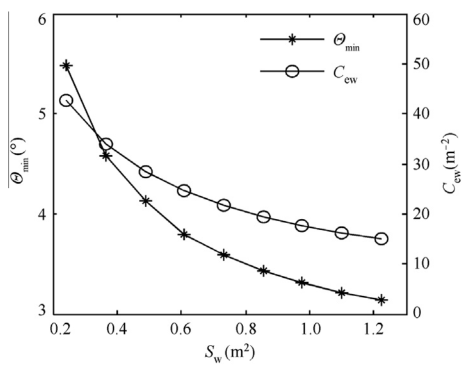

Fig. 9 Variation of Θ_{min} and C_{ew} with different S_w.

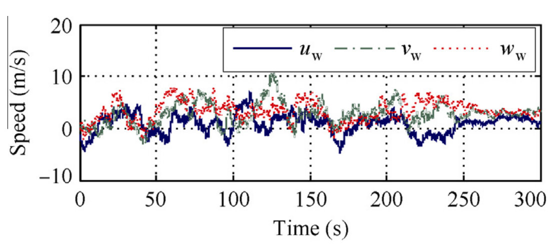

Fig. 10 Velocity of wind influence.

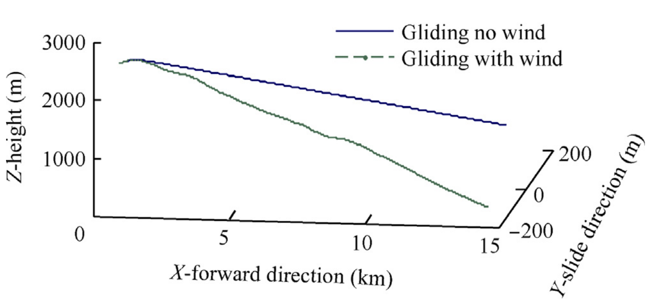

Fig. 11 AL-AUV gliding track with or without wind influence.

Defining AUV gliding angle Θ and wing's coefficient of ex-range efficiency C_{ew} as follows:

$$\Theta = \alpha - \Theta_B \tag{6}$$

$$C_{ew} = 1/(S_w \tan\Theta) \tag{7}$$

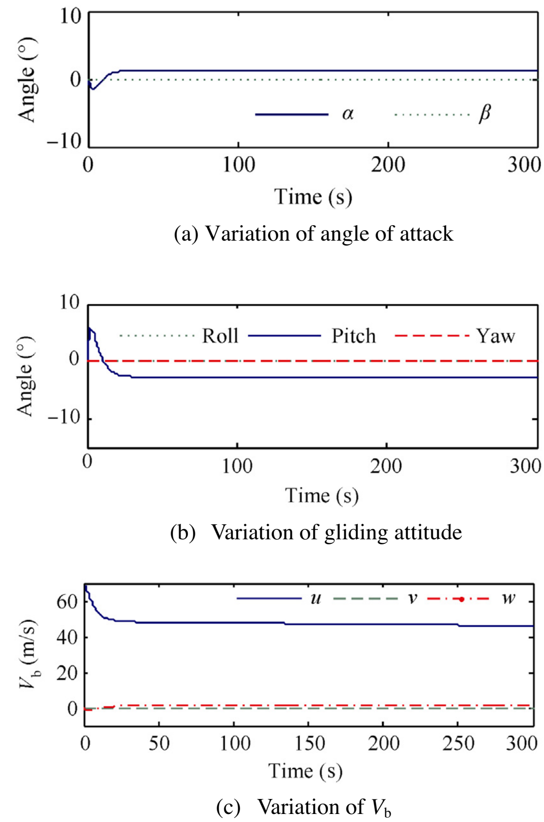

(a) Variation of angle of attack

(b) Variation of gliding attitude

(c) Variation of V_b

Fig. 12 AUV dynamic characteristic without wind influence.

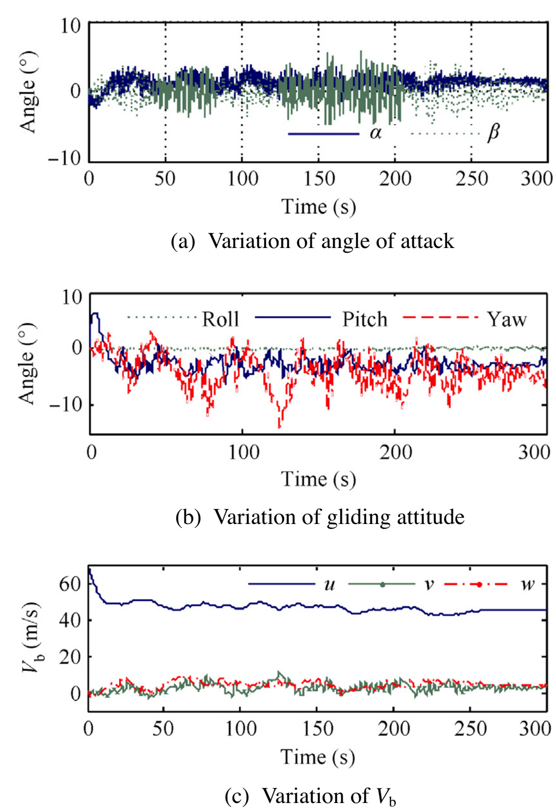

(a) Variation of angle of attack

(b) Variation of gliding attitude

(c) Variation of V_b

Fig. 13 AUV dynamic characteristics with wind influence.

with gliding distance in horizon

$$R_X = C_{ew} S_w H \tag{8}$$

then the variation of gliding angle Θ with the change of α_{set} and S_w is plotted in Fig. 8, which indicates that an optimal exists for each area wing to let AUV be steady at the minimal gliding angle. Processed the simulation data to search out minimal steady gliding angle Θ and the corresponding setting angle of each wing area, and then calculated each point's efficiency coefficient (see Fig. 9). The figure clearly shows that the minimal gliding angle Θ_{min} rapidly decreases with the increase of wing area, which enhances AUV gliding range, meanwhile the decrease of wing's ex-range efficiency coefficient weakens system stability and delays the stabilize time. Compromising the AL-AUV dynamic and steady characteristics, an eclectic wing area was selected with $S_w = 0.489\ m^2$ and the corresponding setting angle $\alpha_{set} = 2.7°$.

5.2. 6DOF simulation with wind influence

To prove the reliability and effectivity of the method mentioned in Section 5.1 on wing design and selection, a group of comparative 6DOF simulation of high altitude AL-AUV with the above-selected wing area and initial angle fitting on AUV body was completed. And the simulated gliding air environment was set to be idealized windless or with Dryden wind. The wind influence, shown in Fig. 10, was provided by a wind module built on Dryden atmospheric turbulence model.[21]

The gliding trajectories of AL-AUV with and without wind influence (see Fig. 11) clearly indicate that the AUV with selected wing area and initial wing fitting angle on body is extensively steady and able to glide a long distance from launch point with a sharp gliding angle (bold solid track), and the track is quavering in vertical direction and yawing in slide direction (fine dash track).

Comparing the AUV's states of angle of attack, attitude and velocity varying with time in different environments (Cases with or without wind influence are respectively shown in Figs. 12 and 13), the AUV gliding dynamic characteristics were obtained. The gliding velocity of AUV in wind influence was approximately kept equal with windless gliding velocity and a slight damping. Whereas the angle of attack and attitude angle at designed steady gliding stage were obviously affected by the damping wind influence, which gravely weakened the high-altitude AL-AUV's ability of extending range. Hence, a large-scale self-adaptable or robust controller is extraordinarily requisite for dominating the deflection angle of rudders at AUV tail to keep the gliding attitude and angle of attack approximate to the designed optimal angle of given wing parameter or dictated angle of navigation and guidance module. Because of the limitation of paper length, the design of self-adaptable or robust controller will be devotedly investigated and discussed in further study.

6. Conclusions

The above simulation results illustrate that the introduced method on the selection of wing parameters and gliding simulation using the established simulation platform for given AUV is accurate and practically valuable. Especially for the AL-AUV's design, an appropriate pair of wings and optimal wing's initial setting angle could be selected for any AUV and desired gliding angle.

References

1. Bellingham JG. Platforms: autonomous underwater vehicles. In: Steele J, Turekian K, Thorpe S, editors. *Encyclopedia of ocean sciences*. 2nd ed. San Diego, CA: Academic Press; 2009. p. 473–84.
2. Jun BH, Park JY, Lee FY, Lee PM, Lee CM, Kim K, et al. Development of the AUV ISiMI and a free running test in an ocean engineering basin. *Ocean Eng* 2009;**36**(1):2–14.
3. Prestero T. Development of a six-degree of freedom simulation model for the REMUS autonomous underwater vehicle. *OCEANS, MTS/IEEE conference and exhibition*; 2001 Nov. 5–8; 2001. p. 450–5.
4. Roe SM. Numerical and experimental analysis of initial water impact of an air dropped REMUS AUV [dissertation]. Massachusetts: Massachusetts Institute of Technology; 2005.
5. Brown N. Long drop for US torpedoes. *Jane's Defence Weekly* 2006;363–4.
6. Brown N. HAAWC glides through wind tunnel trials. *Jane's Navy International* 2006;**111**(9):17–8.
7. Annati M. Anti-submarine weapons-the state of the art. *Mil Technol* 2008;**32**(8):78–91.
8. Alvare A. Redesigning the SLOCUM glider for torpedo tube launching. *IEEE J Oceanic Eng* 2010;**35**(4):984–91.
9. Higgins E. High altitude air-deployed autonomous underwater vehicles [dissertation]. Southampton: University of Southampton; 2007.
10. Stevenson P, Mcphail SD, Tsimplis M, Higgins E. Air launched platforms – a new approach for underwater vehicles. *OCEANS 2009-EUROPE*; 2009 May 11–14. Bremen: IEEE; 2009. p. 1–8.
11. Pan G, Wu WH, Mao ZY, Huang Q. Key technologies about complete trajectory simulation for high altitude long-range gliding torpedo. *Torpedo Technol* 2009;**17**(4):10–5 [Chinese].
12. Zhu XY, Song BW, Mao ZY, Wu WH. Aerodynamic parameter calculation and aerodynamic characteristic analysis of high-altitude gliding UUV. *Comput Simul* 2011;**28**(5):179–83 [Chinese].
13. Song BW, Du XX, Meng R, Li JW, Shao C. Numerical simulation of water entry impact forces for air-launched mine. *Torpedo Technol* 2008;**16**(3):6–8 [Chinese].
14. Wang YH, Shi XH. Modeling and simulation analysis of oblique water-entry impact dynamics of air-dropped torpedo. *Comput Simul* 2009;**26**(1):46–9 [Chinese].
15. Pan CJ, Guo YQ. Design and simulation of high altitude air-launched automatic underwater vehicles. *Appl Mech Mater* 2011;**128–129**:1386–91.
16. Prestero T. Verification of a six-degree of freedom simulation model for the REMUS autonomous underwater vehicle [dissertation]. Massachusetts: Massachusetts Institute of Technology; 2001.
17. Fossen TI, Fjellstad O. Nonlinear modelling of marine vehicles in 6 degrees of freedom. *J Math Model Syst* 1995;**1**(1):17–27.
18. Fossen TI. *Guidance and control of ocean vehicles*. New York: John Wiley & Sons; 1996.
19. Escareño J, Sanchez A, Garcia O, Lozano R. Modeling and global control of the longitudinal dynamics of a coaxial convertible mini-UAV in hover mode. *J Intell Rob Syst* 2009;**54**(1–3):261–73.
20. Tuzcu I, Marzocca P, Cestino E, Romeo G, Frulla G. Stability and control of a high-altitude long-endurance UAV. *J Guid Control Dyn* 2007;**30**(3):713–21.
21. Zhao ZY, Xiao YL, Shi YJ. A digital simulation technique for Dryden atmospheric turbulence model. *J Aeronaut* 1986;**7**(5):433–43 [Chinese].

Pan Changjun received B.S. degree from Northwestern Polytechnical University in 2005. Now he is a Ph.D. student in the same university. His main research interests are control and simulation of air-launched autonomous underwater vehicles and high altitude anti-submaine warfare (ASW).